Multiple spatially distinct types of facultative heterochromatin on the human inactive X chromosome

Brian P. Chadwick and Huntington F. Willard*

Institute for Genome Sciences and Policy and Department of Molecular Genetics and Microbiology, Duke University, Durham, NC 27708

Communicated by Melvin M. Grumbach, University of California School of Medicine, San Francisco, CA, October 28, 2004 (received for review August 16, 2004)

Heterochromatin is defined classically by condensation throughout the cell cycle, replication in late S phase and gene inactivity. Facultative heterochromatin is of particular interest, because its formation is developmentally regulated as a result of cellular differentiation. The most extensive example of facultative heterochromatin is the mammalian inactive X chromosome (Xi). A variety of histone variants and covalent histone modifications have been implicated in defining the organization of the Xi heterochromatic state, and the features of Xi heterochromatin have been widely interpreted as reflecting a redundant system of gene silencing. However, here we demonstrate that the human Xi is packaged into at least two nonoverlapping heterochromatin types, each characterized by specific Xi features: one defined by the presence of Xi-specific transcript RNA, the histone variant macroH2A, and histone H3 trimethylated at lysine 27 and the other defined by H3 trimethylated at lysine 9, heterochromatin protein 1, and histone H4 trimethylated at lysine 20. Furthermore, regions of the Xi packaged in different heterochromatin types are characterized by different patterns of replication in late S phase. The arrangement of facultative heterochromatin into spatially and temporally distinct domains has implications for both the establishment and maintenance of the Xi and adds a previously unsuspected degree of epigenetic complexity.

Barr body | X inactivation | X-inactive-specific transcript

X inactivation is a developmentally regulated process whereby all but one X chromosome per cell are genetically silenced in female mammals to equalize the levels of X-linked gene expression between the sexes (1). Although the early stages of X inactivation have been extensively investigated (2, 3), less well understood is the mechanism by which this complex state is stably maintained throughout subsequent somatic cell divisions.

Several features distinguish the mammalian inactive X chromosome (Xi) from the active X chromosome in the same nucleus, including the nonrandom distribution of histone variants (4, 5), covalent histone modifications (6–11), and delayed replication in S phase (12, 13) that occurs in a highly ordered and cell type-specific pattern (14–16). The association in cis of the Xi-specific transcript (XIST) (17) is the only known unique epigenetic feature of the Xi, because other features are shared, at least to some degree, with other heterochromatic regions of the genome.

Xi heterochromatin is characterized by histone H3 dimethylated at lysine 9 (H3DimK9) (8, 9) and trimethylated at lysine 27 (H3TrimK27) (10, 11), both of which are acquired early during random X inactivation (10, 11, 18, 19) and are achieved by histone methyltransferase enzymes (HMTase) (20). The HMTase responsible for establishing H3TrimK27 at the Xi is the mammalian homologue of *Drosophila enhancer of zeste* gene, *EZH2* (10, 11). *EZH2* is also involved in silencing of homeotic genes, germline development, and stem cell pluripotency (21), thus establishing a mechanistic link between X inactivation and other epigenetic regulatory systems. To date, the HMTase responsible for H3DimK9 at the Xi is unknown.

Several methylated forms of histone H3 at K9 provide a docking site for the chromodomain of heterochromatin protein 1 (HP1) *in vitro* (22–24). However, *in vivo*, HP1 is largely found at pericentric heterochromatin that are defined by the trimethylated form of histone H3 (H3TrimK9) (25), a modification required for HP1 targeting (24). Given that HP1 is found at elevated levels on the human Xi (6) in addition to pericentric heterochromatin, H3TrimK9, in addition to H3DimK9, may also be a feature of X inactivation.

Although considerable attention has been focused on the relative timing and roles of these features during establishment of the Xi heterochromatic state early in development (26), once that epigenetic state is established, they have been widely considered to be redundant (27–31). One prediction of the epigenetic redundancy model is that the features of facultative heterochromatin should colocalize on the Xi in somatic cells. In the present study, we have tested this prediction by examining the spatial arrangement of H3TrimK9 and H3TrimK27 on the human Xi and relating each to the distribution of other features of the Xi and the pattern of replication in late S phase.

Experimental Procedures

Cell Culture. The cell lines that were used included T-3352, a female human primary fibroblast strain; RPE1, a female human telomerase-immortalized cell line derived from the retinal pigment epithelial cell line RPE-340 (catalog no. C4000-1, Clontech); and HME1, a female human telomerase-immortalized cell line derived from a mammary epithelial cell line (catalog no. C4002-1, Clontech). Cells were maintained as described in ref. 32.

Antibodies. Rabbit anti-H3TrimK9 antibodies were obtained from Abcam (Cambridge, U.K.; catalog no. ab8898) and Upstate Biotechnology (Lake Placid, NY; catalog no. 07-523). Both antibody sources gave indistinguishable patterns of distribution on the Xi, both at metaphase and interphase. Rabbit anti-histone H4 trimethylated at lysine 20 (H4TrimK20) and mouse monoclonal anti-H3TrimK27 antibodies were obtained from Abcam (catalog nos. ab9053 and ab60002, respectively). Mouse monoclonal antibodies to BrdUrd conjugated to fluorescein were obtained from Roche (catalog no. 1-202-693). Mouse monoclonal antibodies specific to human HP1 gamma were obtained from Chemicon (catalog no.

Freely available online through the PNAS open access option.

Abbreviations: H3DimK9, histone H3 dimethylated at lysine 9; H3TrimK9, histone H3 trimethylated at lysine 9; H3TrimK27, histone H3 trimethylated at lysine 27; H4TrimK20, histone H4 trimethylated at lysine 20; HP1, heterochromatin protein 1; Xi, inactive X chromosome; XIST, X-inactive-specific transcript.

*To whom correspondence should be addressed at: Institute for Genome Sciences and Policy, Center for Interdisciplinary Engineering, Medicine, and Applied Sciences, Room 2379, Box 3382, 101 Science Drive, Durham, NC 27708. E-mail: willa009@mc.duke.edu.

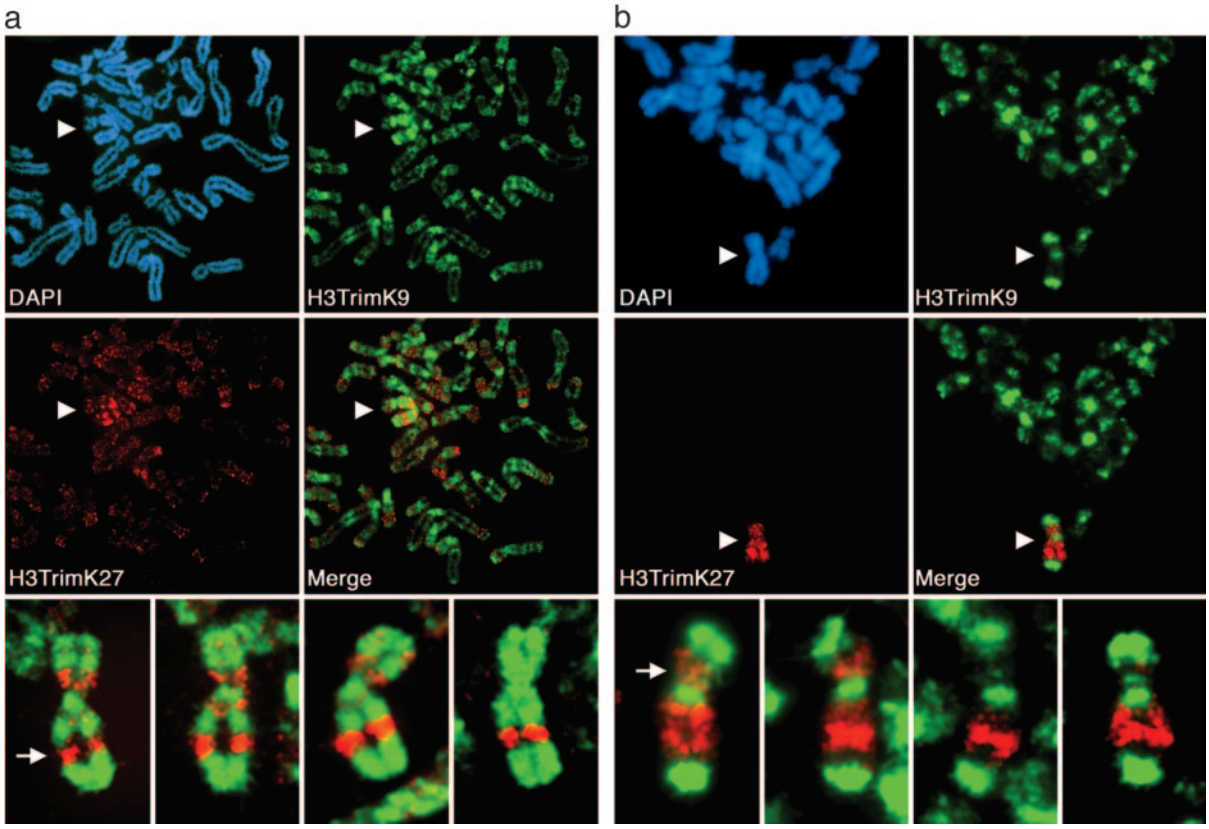

Fig. 1. Spatial relationship of two major Xi heterochromatin types at metaphase. Images represent typical distributions obtained from three independent female cell lines. (*a*) Partial metaphase spread of RPE1 cells showing the spatial distribution of H3TrimK9 (green, FITC) and H3TrimK27 (red, rhodamine) and four additional higher-magnification images of the Xi showing the merged H3TrimK9 and H3TrimK27 distributions. The white arrow indicates the major H3TrimK27 band centered at Xq23. (*b*) Distributions of H3TrimK9 and H3TrimK27 in HME1 cells. The location of the Xi in the partial metaphase spreads is indicated by white arrowheads. The white arrow indicates the major H3TrimK27 band centered at Xp11. All images were obtained by indirect immunofluorescence.

MAB3450). Rabbit anti-macroH2A1 antibodies were described in ref. 4. Fluoresceinated secondary antibodies were obtained from Jackson ImmunoResearch.

Immunofluorescence and Fluorescence *in Situ* Hybridization. Immunofluorescence and RNA FISH were carried out essentially as described in ref. 32. Images were collected by using OPENLAB software (Improvision, Lexington, MA) with an ORCA-ER camera (Hamamatsu Photonics, Hamamatsu City, Japan) on a Zeiss Axiovert 200M.

Peptide Competition. To confirm antibody specificity for H3TrimK9 and H3TrimK27, immunostaining was performed with and without preincubating antibodies with various methylated forms of H3 peptides. Peptides representing H3DimK9 (catalog no. ab1772), H3TrimK9 (catalog no. ab1773), H3DimK27 (catalog no. ab1781), and H3TrimK27 (catalog no. ab1782) were obtained from Abcam. Blocking was achieved by preincubating antibodies in a solution of peptides at 10 μg/ml in 1× PBS supplemented with 1% BSA and 0.1% Tween 20 at room temperature for 2 h before staining. Xi-specific signals were only abolished when antibodies were first blocked with the corresponding trimethylated H3 peptide (data not shown). In contrast, no discernable differences in staining patterns were observed for anti-H3TrimK9 or anti-H3TrimK27 after blocking against the opposing epitope. Thus, we have validated that the commercially available antisera are specific for the claimed epitopes.

Late Replication Assay. Cells were incubated in the presence of BrdUrd (Sigma) between 2 and 6 h before arrest in mitosis and harvest (14). To analyze late replication patterns characteristic of the Xi, metaphase chromosomes were prepared as described in ref. 32 and counterstained for the distribution of H3TrimK9 or H3TrimK27 relative to BrdUrd incorporation.

Results and Discussion

At Metaphase, the Xi Is Characterized by Alternating Bands of Differentially Methylated Forms of Histone H3. Methylation of histone H3 at K9 and K27 are characteristic markers of the Xi (8–11). At metaphase, H3DimK9 is distributed throughout the Xi (6, 8, 9). To extend these studies, we analyzed the distribution of H3TrimK9 and H3TrimK27 on the human Xi by using antibodies shown to be specific for each epitope (see *Experimental Procedures*). Strikingly, both H3TrimK9 and H3TrimK27 are nonrandomly distributed along the Xi at metaphase and locate to reproducible bands (Fig. 1). Furthermore, the distributions of H3TrimK9 and H3TrimK27 at metaphase do not overlap; they occupy alternating bands along the length of the Xi, and signal overlap was not detected in 300 metaphase spreads examined from three independent female cell lines (Table 1 and Fig. 1). In fact, even elsewhere throughout the genome, other regions of H3TrimK27 immunostaining appear distinct from that of H3TrimK9 (Fig. 1*a*), suggesting that this spatial segregation of the two modified forms of histone H3 is a common feature of heterochromatin in general. The degree of enrichment of H3TrimK9 and H3TrimK27 on the Xi also differs. Although H3TrimK27 is heavily enriched on the Xi (e.g., Fig. 1), H3TrimK9 staining is also observed on many autosomes and the active X chromosome (in addition to its strong localization to pericentromeric regions).

Table 1. Spatial arrangement of different heterochromatin features of the human Xi at interphase and metaphase

Feature	No. of cells (cell lines)	Metaphase or interphase analysis	Cells/chromosomes examined, %		
			Complete overlap	Partial overlap	No overlap
H3TrimK9 vs. H3TrimK27	300 (3)	Metaphase	0.0 ± 0.0	0.0 ± 0.0	100.0 ± 0.0
macroH2A1 vs. H3TrimK27	184 (2)	Metaphase	95.0 ± 7.1	5.0 ± 7.1	0.0 ± 0.0
H3TrimK9 vs. H3TrimK27	600 (3)	Interphase	8.4 ± 12.6	31.8 ± 20.1	59.8 ± 31.9
H3TrimK9 vs. XIST	600 (3)	Interphase	3.2 ± 2.5	14.0 ± 5.3	82.8 ± 7.8
H3TrimK27 vs. XIST	600 (3)	Interphase	92.0 ± 9.9	8.0 ± 9.9	0.0 ± 0.0

Although each of the cell lines investigated demonstrated a clear nonoverlapping distribution of H3TrimK9 and H3TrimK27, variation was observed in the frequency of particular bands among different cell lines (Fig. 1, compare *a* with *b*). For example, in a detailed band by band analysis of 50 metaphase Xi from three independent cell lines, the intense band of H3TrimK27 centered at Xq23 was always observed (see Fig. 1*a Bottom*, leftmost image), whereas the band centered around Xp11 was more frequently a feature of the HME1 (see Fig. 1*b Bottom*, leftmost image) (39/50 metaphase Xi) cell line than either the RPE1 (10/50 metaphase Xi) or T-3352 (1/50 metaphase Xi) cell lines. Similar variation among cell lines was also observed for H3TrimK9 staining (data not shown). These data suggest that the composition of Xi heterochromatin varies between cell lines or cell types. Interestingly, this heterogeneity is similar to that noted several decades ago for the replication timing of different regions of the Xi among different cell types (15, 16) (see below). Of note, whereas H3TrimK9 and H3TrimK27 clearly cover most of the Xi, some regions, particularly the intervals between the two defined chromatin types, are not defined by either modification. It may be that an additional type(s) of Xi heterochromatin exists at these regions, the composition of which is currently unclear.

The banding patterns observed for H3TrimK9 and H3TrimK27 are reminiscent of those observed previously for macroH2A, a variant of core histone H2A that is enriched on the Xi (4, 5). *In vitro* data indicate a functional role for macroH2A in transcriptional regulation through the promotion of higher-order chromatin structure, obstruction of transcription factor access, and a reduced chromatin remodeling competence (33, 34). At interphase, the association of macroH2A with the Xi appears as an intensely staining mass, referred to as a macro chromatin body (5). At metaphase, macroH2A is not distributed uniformly along the chromosome, but is restricted to distinct regions on the Xi (32). To examine directly the relationship between macroH2A and H3Trim27 on the Xi, metaphase chromosomes were doubly immunostained with appropriate antisera. Notably, the general banding pattern of H3TrimK27 was indistinguishable from that of macroH2A (Table 1), and a more detailed band-by-band analysis revealed a near-perfect correlation between H3TrimK27 and macroH2A bands (93–100%, $n = 50$ for two independent cell lines). It has been reported that elevated levels of macroH2A on the Xi may in fact reflect an overall increase in the density of nucleosomes (35). Given the data reported here, such a higher nucleosome density at the Xi would be restricted to those defined bands correlating with regions of H3TrimK27, suggesting that H3TrimK27 may in part mediate inhibition of gene expression in heterochromatin by increasing local nucleosome densities.

Asynchronous Replication of the Xi Correlates Directly with Heterochromatin Composition. A shift of replication timing to late in S phase is one of the earliest hallmarks of X inactivation during development (26, 36) and has long been used as a defining feature of the human Xi (12, 13). To investigate the relationship between the characteristic pattern of Xi replication in late S phase and the two types of facultative heterochromatin reported here, we compared the replication pattern of the Xi with the metaphase banding of H3TrimK9 and H3TrimK27 in two independent cell lines. When cells were labeled with BrdUrd in the last 2–3 h of S phase, a clear overlap was seen between the labeled DNA and H3TrimK9-containing heterochromatin (100% of metaphase spreads, $n = 200$), but not H3TrimK27-containing heterochromatin (only 9% of metaphase spreads, $n = 197$) (Fig. 2). Labeling cells 2 h earlier in mid to late S phase was sufficient to incorporate BrdUrd into H3TrimK27-containing heterochromatin (data not shown). Thus, the two types of Xi heterochromatin are temporally and spatially distinct, with only H3TrimK9-modified heterochromatin showing the classic feature of replication in very late S phase.

The Spatially Segregated Arrangement of Xi Heterochromatin Is Maintained at Interphase. A defining feature of the human Xi in interphase is the presence of the heterochromatic Barr body at the periphery of the nucleus (37). We thus investigated whether the two types of heterochromatin detected at metaphase remain spatially distinct in interphase or whether they intermix during compaction of the Xi into the Barr body. Fig. 3 clearly shows that H3TrimK9 and H3TrimK27 occupy distinct territories at interphase, with nearly 60% of cells showing no overlap between the two signals (Table 1), suggesting that different regions of the Xi fold into separate, coherent domains within the Barr body. To extend these findings, we next examined several other features of Xi chromatin in interphase.

Mouse Xist RNA associates with the Xi in a banded pattern (38, 39). Although human XIST RNA does not remain associated with the Xi at metaphase (40), it does label the Barr body at interphase (41). Thus, we investigated the relationship of XIST RNA at interphase to the two types of heterochromatin within the Barr body. As shown in Fig. 3 and Table 1, XIST RNA clearly associates with H3TrimK27-defined heterochromatin and not with H3TrimK9 heterochromatin. In agreement with the metaphase banding (Table 1), the XIST/H3TrimK27 territory is also defined by macroH2A (Fig. 3).

We have previously shown that HP1 is a feature of the human Xi (6). At interphase, elevated levels of HP1 are coincident with H3TrimK9 in the Barr body (Fig. 3), which is consistent with H3TrimK9 providing a docking site for HP1 (22, 24). Notably, this same territory is defined by elevated levels of histone H4TrimK20 (Fig. 3), consistent with data indicating that induction of H4TrimK20 is intimately linked to establishment of H3TrimK9 patterns in mammalian pericentric heterochromatin (42). However, HP1 and H4TrimK20 are not consistent features of the Xi in all human cell lines (data not shown). It is tempting to posit that this variation may reflect the extent of H3TrimK9 on the Xi in a given cell line. For example, the different staining for H3TrimK9 seen in the HME1 and RPE-1 cell lines (Fig. 1) correlates well with the levels of HP1 staining; although HP1 is readily detected at the RPE1 Xi at interphase (6), this is not the case for HME1, in which

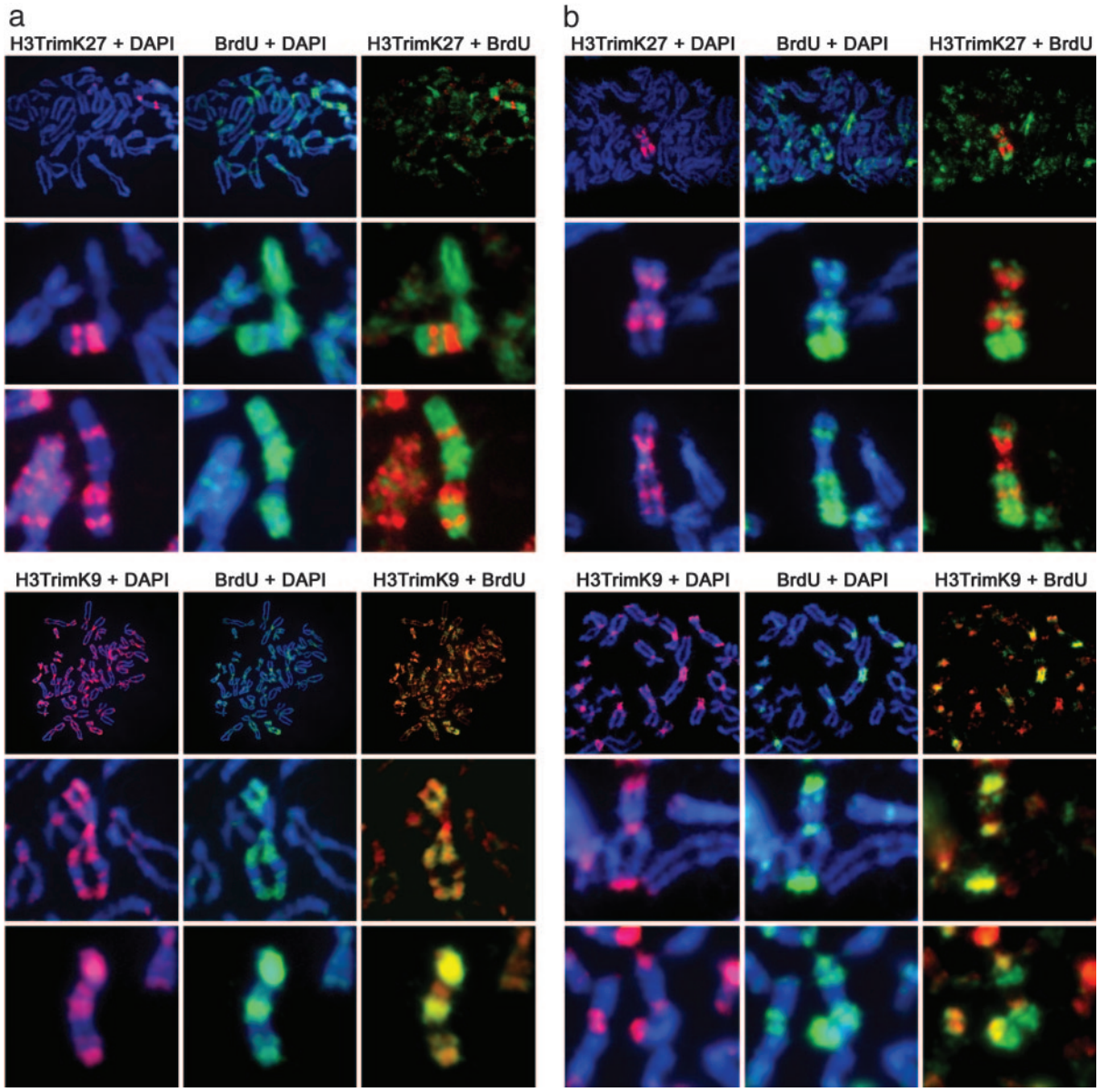

Fig. 2. Correlation of H3TrimK27 (*a Upper* and *b Upper*) and H3TrimK9 (*a Lower* and *b Lower*) heterochromatin with the Xi replication pattern. (*a*) Metaphase chromosomes prepared from RPE1 cells that were incubated with BrdUrd for 4 h before metaphase arrest (corresponding approximately to the last 2 h of S phase). (*b*) Metaphase chromosomes prepared from HME1 cells that were incubated with BrdUrd for 3 h before metaphase arrest (corresponding approximately to the last 2 h of S phase). In each section, *Top* shows a partial metaphase spread, whereas *Middle* and *Bottom* show the Xi from independent spreads at higher magnification.

HP1 is rarely detected at the Xi (data not shown). These data support a role for H3TrimK9 in providing the framework for HP1-mediated higher-order heterochromatin formation (43).

Together, the data here indicate that the Xi is composed of at least two major types of facultative heterochromatin that are partitioned within the interphase nucleus, one characterized by H3TrimK27, XIST RNA, and macroH2A and the other characterized by H3TrimK9, HP1, and H4TrimK20. These data indicate that packaging of the Xi into the Barr body follows a prescribed pattern of folding that maintains the spatial distinction of the two types of heterochromatin apparent at metaphase. This raises the question of how the Xi might transition between the distinct bands of H3TrimK9 and H3TrimK27/macroH2A seen at metaphase and the spatially segregated territories observed at interphase. To account for these patterns, we propose that the two chromatin types are marked epigenetically by either H3TrimK9 or macroH2A throughout the cell cycle. After mitosis, these epigenetic marks would then initiate association with other features of each heterochromatin type (Fig. 4), HP1 associating with H3TrimK9-defined heterochromatin (44) and XIST RNA, newly synthesized from the X inactivation center (40, 41), associating with macroH2A-defined heterochromatin. An important feature of the model is that the spreading of XIST RNA in *cis* along the Xi is guided (and perhaps constrained) by local folding of different regions of the X chromosome, thus effectively skipping regions of H3TrimK9 heterochromatin by virtue of the spatial dichotomy of the chromosome (Fig. 4). In addition to explaining the bipartite nature of the Barr body, this model could explain the variation observed in X-inactivation spread into autosomal material in different X–autosome translocations (44–46). In such a model, the extent of heterochromatin spread into adjacent autosomal chromatin would be

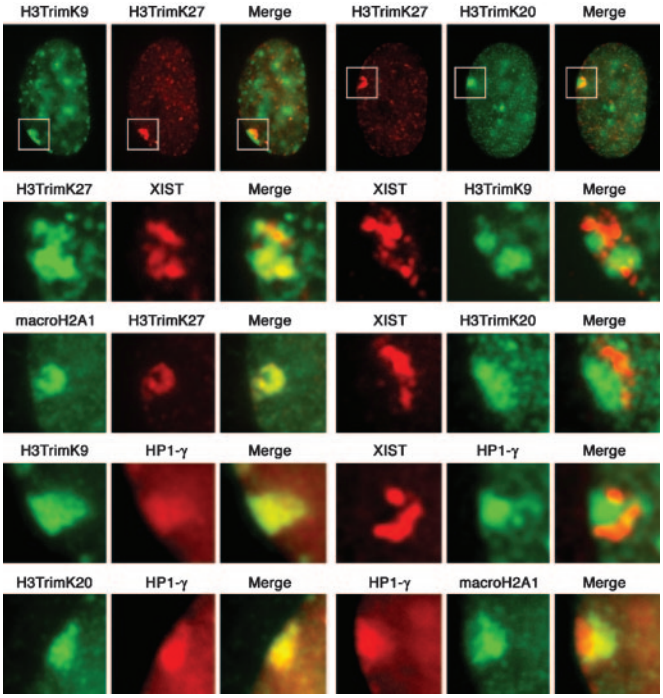

Fig. 3. Characterization of Xi chromatin territories at interphase. All images are of the RPE1 cells and represent typical observations made in at least four independent female cell lines. The white box in each interphase nucleus (top row) represents the Barr body region examined at higher magnification in the other images below. The feature examined by indirect immunofluorescence is labeled above each image. Overlapping red and green signals appear yellow.

determined in part by the type of heterochromatin in which the breakpoint occurred. Whether this banded and alternating epigenetic packaging of the Xi reflects underlying regional differences in the X chromosome genomic sequence and/or whether it signals the as yet incompletely understood nature of chromatin folding within subnuclear compartments is unknown at present.

Implications of Distinct Heterochromatin Territories at the Xi. In this report, we have demonstrated that the human Xi is packaged into several alternative types of heterochromatin that are spatially distinct. These findings raise several important questions regarding X inactivation and its relationship to other examples of epigenetic silencing, both in mammals and other systems. In light of previous observations of the Barr body and its colocalization with XIST RNA, macroH2A, and various modifications of histone H3 (5, 8–11, 40), it is important to reconcile our findings with models that assume a uniform type of facultative heterochromatin, with particular emphasis on the redundant nature of X inactivation (27, 28, 30, 47, 48). Such models have interpreted the stability of the silenced state as a suggestion that the loss of one feature would be compensated by additional epigenetic features. Our data indicate, however, that the apparent redundant nature of X inactivation more likely reflects the dynamic ability of other heterochromatic

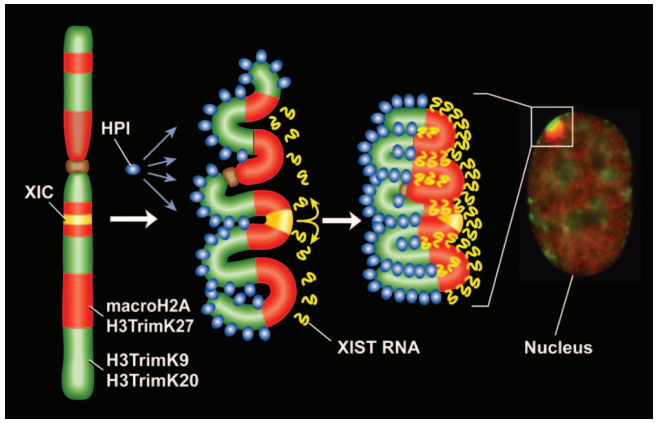

Fig. 4. Schematic model showing how heterochromatin of the Xi could transition between metaphase and interphase to be organized into the two nonoverlapping heterochromatin territories and to explain how XIST RNA could rapidly spread in cis outward from the X inactivation center (XIC) along only part of the Xi. See main text for details.

features to spread into compromised regions to maintain the silenced state. A precedent for such a model is the apparent rescue of pericentric constitutive heterochromatin by features of facultative heterochromatin. In Suv39h double-mutant mice, H3TrimK9 at pericentric heterochromatin is lost but is replaced by acquisition of H3TrimK27 (25).

The organization of the Xi into major spatially distinct types of heterochromatin adds a new level of complexity to our understanding of X inactivation. This arrangement may reflect an evolutionary adaptation to assist in mediating heterochromatin over long distances as is uniquely necessary for chromosome-wide gene silencing in X inactivation. The major consequence of X inactivation is the transcriptional silencing of genes on the Xi (1). However, gene silencing on the human Xi is not complete, because numerous genes escape inactivation and are expressed from the Xi to differing degrees (49). Notably, genes that escape inactivation are nonrandomly interspersed along the length of the Xi, with the majority located on the short arm of the X chromosome, Xp (49), some of which are clustered together into multigenic domains (50). Although there is no obvious correlation between the banding patterns described here and the underlying pattern of X inactivation, it will be important to evaluate at the local level what effect such an arrangement of Xi heterochromatin might have on the stability of gene silencing. One might anticipate that H3TrimK27/macroH2A/XIST-defined heterochromatin is less effective at silencing gene expression than the late-replicating, highly conserved H3TrimK9/HP1/H4TrimK20 heterochromatin, as it is deficient for key components shown in other systems to be necessary for maintaining gene silencing (51). Consequently, escape from inactivation might be more frequently a feature of one form of heterochromatin than the other.

This work was supported by National Institutes of Health Grant GM45441 (to H.F.W.).

1. Lyon, M. F. (1961) *Nature* **190,** 372–373.
2. Avner, P. & Heard, E. (2001) *Nat. Rev.* **2,** 59–67.
3. Plath, K., Mlynarczyk-Evans, S., Nusinow, D. A. & Panning, B. (2002) *Annu. Rev. Genet.* **36,** 233–278.
4. Chadwick, B. P. & Willard, H. F. (2001) *Hum. Mol. Genet.* **10,** 1101–1013.
5. Costanzi, C. & Pehrson, J. R. (1998) *Nature* **393,** 599–601.
6. Chadwick, B. P. & Willard, H. F. (2003) *Hum. Mol. Genet.* **12,** 2167–2178.
7. Jeppesen, P. & Turner, B. M. (1993) *Cell* **74,** 281–289.
8. Boggs, B. A., Cheung, P., Heard, E., Spector, D. L., Chinault, A. C. & Allis, C. D. (2002) *Nat. Genet.* **30,** 73–76.
9. Peters, A. H., Mermoud, J. E., O'Carroll, D., Pagani, M., Schweizer, D., Brockdorff, N. & Jenuwein, T. (2002) *Nat. Genet.* **30,** 77–80.
10. Plath, K., Fang, J., Mlynarczyk-Evans, S. K., Cao, R., Worringer, K. A., Wang, H., de la Cruz, C. C., Otte, A. P., Panning, B. & Zhang, Y. (2003) *Science* **300,** 131–135.
11. Silva, J., Mak, W., Zvetkova, I., Appanah, R., Nesterova, T. B., Webster, Z., Peters, A. H., Jenuwein, T., Otte, A. P. & Brockdorff, N. (2003) *Dev. Cell* **4,** 481–495.
12. Gilbert, C. W., Muldal, S., Lajthal, L. G. & Rowley, J. (1962) *Nature* **195,** 869–873.

13. Morishma, A., Grumbach, M. M. & Taylor, J. H. (1962) *Proc. Natl. Acad. Sci. USA* **48,** 756–763.
14. Willard, H. F. & Latt, S. A. (1976) *Am. J. Hum. Genet.* **28,** 213–227.
15. Willard, H. F. (1977) *Chromosoma* **61,** 61–73.
16. McCaw, B. K. & Latt, S. A. (1977) *Hum. Genet.* **38,** 253–264.
17. Brown, C. J., Ballabio, A., Rupert, J. L., Lafreniere, R. G., Grompe, M., Tonlorenzi, R. & Willard, H. F. (1991) *Nature* **349,** 38–44.
18. Heard, E., Rougeulle, C., Arnaud, D., Avner, P., Allis, C. D. & Spector, D. L. (2002) *Cell* **107,** 727–738.
19. Mermoud, J. E., Popova, B., Peters, A. H., Jenuwein, T. & Brockdorff, N. (2002) *Curr. Biol.* **12,** 247–251.
20. Sims, R. J., III, Nishioka, K. & Reinberg, D. (2003) *Trends Genet.* **19,** 629–639.
21. Cao, R. & Zhang, Y. (2004) *Curr. Opin. Genet. Dev.* **14,** 1–10.
22. Bannister, A. J., Zegerman, P., Partridge, J. F., Miska, E. A., Thomas, J. O., Allshire, R. C. & Kouzarides, T. (2001) *Nature* **410,** 120–124.
23. Jacobs, S. A., Taverna, S. D., Zhang, Y., Briggs, S. D., Li, J., Eissenberg, J. C., Allis, D. & Khorasanizadeh, S. (2001) *EMBO J.* **20,** 5232–5241.
24. Lachner, M., O'Carroll, D., Rea, S., Mechtler, K. & Jenuwein, T. (2001) *Nature* **410,** 116–120.
25. Peters, A. H., Kubicek, S., Mechtler, K., O'Sullivan, R. J., Derijck, A. A., Perez-Burgos, L., Kohlmaier, A., Opravil, S., Tachibana, M., Shinkai, Y., *et al*. (2003) *Mol. Cell* **12,** 1577–1589.
26. Heard, E. (2004) *Curr. Opin. Cell Biol.* **16,** 247–255.
27. Brown, C. J. & Willard, H. F. (1994) *Nature* **368,** 154–156.
28. Csankovszki, G., Panning, B., Bates, B., Pehrson, J. R. & Jaenisch, R. (1999) *Nat. Genet.* **22,** 323–324.
29. Csankovszki, G., Nagy, A. & Jaenisch, R. (2001) *J. Cell Biol.* **153,** 773–784.
30. Mohandas, T., Sparkes, R. S. & Shapiro, L. J. (1981) *Science* **211,** 393–396.
31. Rack, K. A., Chelly, J., Gibbons, R. J., Rider, S., Benjamin, D., Lafreniere, R. G., Oscier, D., Hendriks, R. W., Craig, I. W., Willard, H. F., *et al*. (1994) *Hum. Mol. Genet.* **3,** 1053–1059.
32. Chadwick, B. P. & Willard, H. F. (2002) *J. Cell Biol.* **157,** 1113–1123.
33. Angelov, D., Molla, A., Perche, P. Y., Hans, F., Cote, J., Khochbin, S., Bouvet, P. & Dimitrov, S. (2003) *Mol. Cell* **11,** 1033–1041.
34. Changolkar, L. N. & Pehrson, J. R. (2002) *Biochemistry* **41,** 179–184.
35. Perche, P. Y., Vourc'h, C., Konecny, L., Souchier, C., Robert-Nicoud, M., Dimitrov, S. & Khochbin, S. (2000) *Curr. Biol.* **10,** 1531–1534.
36. Takagi, N. (2003) *Semin. Cell Dev. Biol.* **14,** 319–329.
37. Barr, M. L. & Bertram, E. G. (1949) *Nature* **163,** 676–677.
38. Duthie, S. M., Nesterova, T. B., Formstone, E. J., Keohane, A. M., Turner, B. M., Zakian, S. M. & Brockdorff, N. (1999) *Hum. Mol. Genet.* **8,** 195–204.
39. Mak, W., Baxter, J., Silva, J., Newall, A. E., Otte, A. P. & Brockdorff, N. (2002) *Curr. Biol.* **12,** 1016–1020.
40. Clemson, C. M., McNeil, J. A., Willard, H. F. & Lawrence, J. B. (1996) *J. Cell Biol.* **132,** 1–17.
41. Brown, C. J., Hendrich, B. D., Rupert, J. L., Lafreniere, R. G., Xing, Y., Lawrence, J. & Willard, H. F. (1992) *Cell* **71,** 527–542.
42. Schotta, G., Lachner, M., Sarma, K., Ebert, A., Sengupta, R., Reuter, G., Reinberg, D. & Jenuwein, T. (2004) *Genes Dev.* **18,** 1251–1262.
43. Grewal, S. I. & Elgin, S. C. (2002) *Curr. Opin. Genet. Dev.* **12,** 178–187.
44. White, W. M., Willard, H. F., Van Dyke, D. L. & Wolff, D. J. (1998) *Am. J. Hum. Genet.* **63,** 20–28.
45. Hall, L. L., Clemson, C. M., Byron, M., Wydner, K. & Lawrence, J. B. (2002) *Hum. Mol. Genet.* **11,** 3157–3165.
46. Sharp, A. J., Spotswood, H. T., Robinson, D. O., Turner, B. M. & Jacobs, P. A. (2002) *Hum. Mol. Genet.* **11,** 3145–3156.
47. Singer-Sam, J., Goldstein, L., Dai, A., Gartler, S. M. & Riggs, A. D. (1992) *Proc. Natl. Acad. Sci. USA* **89,** 1413–1417.
48. Gartler, S. M. & Goldman, M. A. (1994) *Dev. Genet. (Amsterdam)* **15,** 504–514.
49. Carrel, L., Cottle, A. A., Goglin, K. C. & Willard, H. F. (1999) *Proc. Natl. Acad. Sci. USA* **96,** 14440–14444.
50. Miller, A. P. & Willard, H. F. (1998) *Proc. Natl. Acad. Sci. USA* **95,** 8709–8714.
51. Maison, C. & Almouzni, G. (2004) *Nat. Rev. Mol. Cell Biol.* **5,** 296–304.